International Journal of Engineering & Technology, 7 (3.2) (2018) 316-321

International Journal of Engineering & Technology

Website: www.sciencepubco.com/index.php/IJET

Research paper



The Stress-Strain State Computer Modelling of Reinforced Masonry Under Local Loading

Nataliia Pinchuk[1]*, Oleksiy Fenko[2], Volodymyr Kyrychenko[3]

[1]*Poltava National Technical Yuri Kondratyuk University*
[2]*Poltava National Technical Yuri Kondratyuk University*
[3]*Poltava National Technical Yuri Kondratyuk University*
**Corresponding Author E-Mail: Natali.Pinchuk.Pntu@Gmail.Com*

Abstract

Reinforced masonry elements stress-strain state modelling allows to define places in which stresses and strains are maximum. It is necessary to pay special attention to these places during experimental investigation. Accepted models of structures are adequate and corresponded to real constructions. Using computer modelling by the finite element method, the finite element size influence on the calculation accuracy is determined. The necessary resources of a personal computer to create and calculate such a model are sufficient and suitable for studying modelled structures stress-strain state. Good convergence of the deformations obtained from the resistive-strain sensors during the experimental investigations and according to the numerical modelling results is received.

Keywords: *numerical computer modelling, reinforced masonry, stress concentration.*

1. Introduction

Computer modelling with commercial software packages (ANSYS, NASTRAN, SCAD, Cosmos, ASKA, LIRA, MONOMAH, etc.) is intended for the stress-strain state (SSS) numerical research on the computer, stability of structures in general and their elements and detection of dangerous stress concentration areas [1]. Such computer modelling allows to reduce the volume of experiments and reduce their cost [2]. Bearing capacity increasing and reducing the deformability of the building structural bearing elements, made from brick preserving the original sizes (that is, the same amount of consumables), is always an urgent task of research work. The aforementioned issues can be partly solved by reinforcing meshes using in masonry [3, 5].

2. The Order of Samples Model Creating and their Analysis

Numerical modelling of SSS is made in NASTRAN system [4, 6-12]. This finite-element analysis program has been recognized as a leader in this field because of the complete overview of the different physical materials nature phenomena which being studied. The training demo version of SDRC-FEMAP 8 / 1a S / N 000-00-00-DEMO-406F-00000000 was used.

The investigated model of reinforcement masonry in plan is 250 × 1050 mm, height is 1050 mm. In this case the mark of brick is M75, mark of mortar is M50. The masonry was reinforced through three rows (225 mm) with reinforcing mesh, the diameter of bars is 4 mm and the size is 50 × 50 mm (see Figure 1).

Geometric models of the studied virtual samples were directly created in the subprogram Femap. The global Cartesian rectangular coordinate system was used in creating of the samples geometry. Initially, a flat cross-section of the masonry explored model was created with the help of straight lines defined by the joint points coordinates. The three-dimensional design model (masonry) was formed by extending the model shape formed in advance by the given direct plane boundary surface. To specify the reinforcing bars, it is necessary to prioritize their direct location in a solid (masonry). For this, the solid body was cut by the planes, at the intersection of which lines for the subsequent placement of reinforcing bars were formed. Checking of geometric characteristics of the created flat section was made: the area, the position of the gravity center, the inertia moments, the resistance moments and the inertia radius relative to the main axes.

Materials of the model (masonry and reinforcing bars characteristics) were separately specified as isotropic. All properties of materials were given in the form of scalar quantities. The value of the materials physical and mechanical characteristics (Jung's elastic modulus E and the coefficient of transverse deformation ν) and the deformation law (σ-ε) were taken in accordance with the current normative documents. During the structures modelling it was assumed that they work in elastic-plastic stage. Therefore, when the materials characteristics were given, two-line dependences between load-deformations were taken into account. For reinforcement of the class Bp-I, the initial elastic modulus $E_s=2\times10^5$ MPa was used, the failure stresses (the conditional reinforcement yield line) σ_s=494 MPa, the deformation $\varepsilon_s=2{,}47\times10^{-3}$; the temporary resistance of the reinforcement σ_u = 659 MPa. For the masonry, the initial elasticity modulus $E_s=2\times10^4$ MPa was given, the failure stresses at the cracks formation moment in the masonry σ_c= 4 MPa, the deformations at this limit $\varepsilon_c=2{,}00\times10^{-4}$.

Copyright © 2018 Authors. This is an open access article distributed under the Creative Commons Attribution License, which permits unrestricted use, distribution, and reproduction in any medium, provided the original work is properly cited.

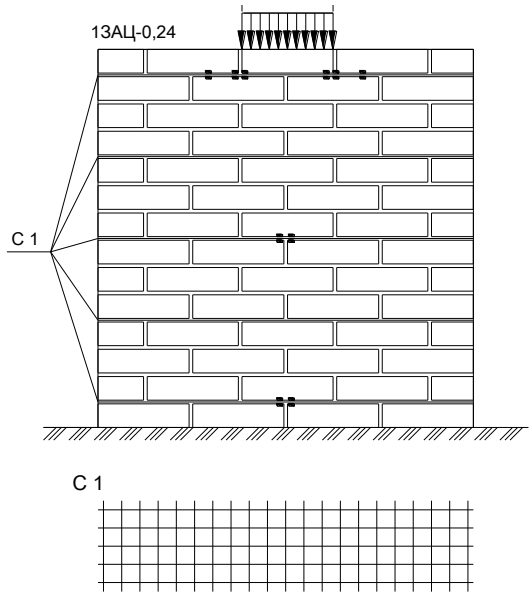


Fig. 1: Constructive scheme of the reinforced masonry investigated model.

According to the analysis results (see Table 1), for the creation of a samples finite element grid, it was decided to use three-dimensional elements of type in solid form of hexahedrons. To create a finite element reinforcing mesh frame and steel structures linear amplification (angles and bands) we used linear elements such as Beam pointing the section shape (Circular Bar or Rectangular Bar) and its size (Diameter and Height or Width). The element side size was taken as 25 mm, which is about 2.5% of the maximum model size (height or length).

Table 1: The results of the masonry model breakdown into various volumetric finite elements

Finite elements size, mm	Type of finite elements	
	tetrahedron	**hexahedron**
10 (1/100·*h*)	748259	160436
25 (1/40·*h*)	151046	19740
50 (1/20·*h*)	35590	3036

After the breakdown of the modeled element details (masonry and reinforcing bars), the finite elements were carried out by combining the matching joints along its length. The finite-element meshes of the model details are shown on figure 2.

The sample was loaded on the upper site at the size of 250 × 250 mm. The sample lower horizontal surface had a hard clamping across the area (see Figure 1).

After a finite-element analysis, a plurality of stress and strain distribution diagrams were obtained for the masonry and reinforcement surface. The most characteristic of them are given below.

Thus, for example, in Figure 3, a-c, the distributions of normal stresses toward the vertical axis z of loading σ_z normal toward the horizontal axis x of the specimen (along its long side) $\boldsymbol{\sigma_x}$ and the tangential shear stress $\boldsymbol{\tau_{zx}}$ in the plane *zx* on the masonry surface of the specimen 13АЦ-0,24. Figure 3, d shows the distribution of stresses in the reinforcing mesh of the sample 13АЦ-0,24.

In addition to the color diagrams showing the stress distribution the color scales specifying the color and the corresponding numerical value of stresses in MPa are shown. The strain distribution diagrams on the surface of the reinforced masonry also show a deformed state from the applied load. Comparison of maximum compressive and tensile stresses values for different types of loading is graphically done (see Figure 6).

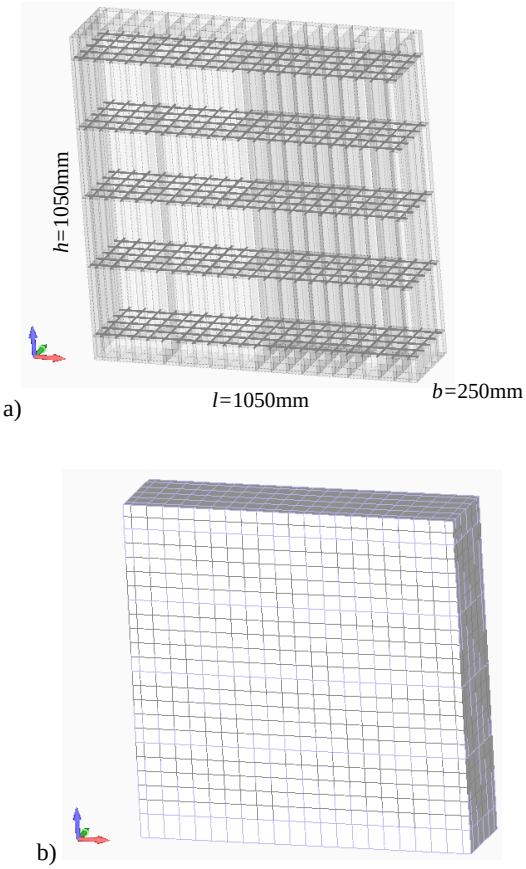


Fig. 2: a) Finite-element mesh of reinforcing bars. b) Finite-element net of masonry block in the form of hexahedrons.

The sample was loaded on the upper site in the size of 250 × 250 mm. The sample lower horizontal surface had a hard clamping across the area (see Figure 1).

The modelling of the stress-strain state was performed for three elements of clay masonry, the size and loading of which corresponded to experiment. The samples differed in the width of the site of the applied loading, as well as the value of the applied failure load. Table 2 lists the value of the applied failure load and the dimensions of the sites to which this load has been applied, according to the sample cipher. Table 3 shows outlines of simulated samples that are similar to experimentally tested specimens (see Figure 3).

After a finite-element analysis, a plurality of stress and strain distribution diagrams were obtained for the masonry and reinforcement surface. The most characteristic of them are given below.

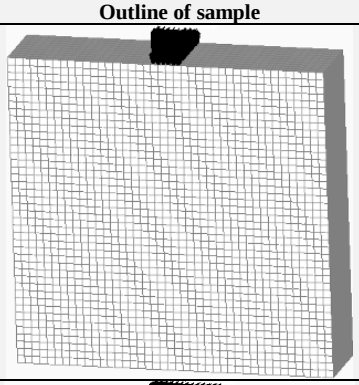
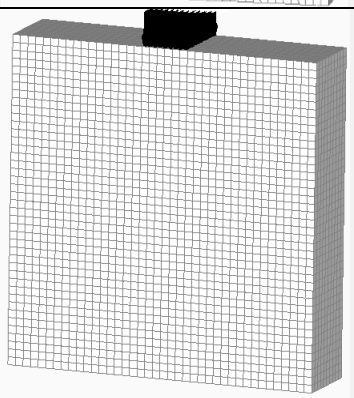
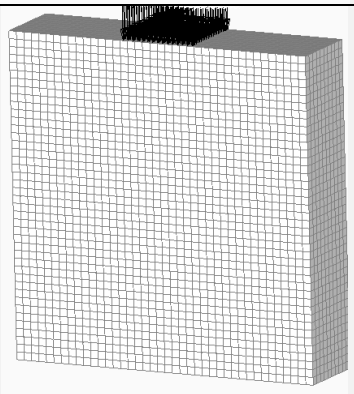
Thus, for example, in Figure 4, a-c, the distributions of stresses which are normal toward the vertical axis z of loading σ_z normal toward the horizontal axis x of the specimen (along its long side) $\boldsymbol{\sigma_x}$ and the tangential shear stress $\boldsymbol{\tau_{zx}}$ in the plane *zx* on the surface of the masonry specimen 13АЦ-0,24. Figure 4, d shows the stresses distribution in the sample 13АЦ-0,24 of reinforcing mesh.

Comparing the received stress values, shown in Figure 6, we can make the following conclusions. The greatest stresses are the normal stress $\boldsymbol{\sigma_z}$ toward the longitudinal axis of loading. Tension of compression is 10-20 times greater than the tensile stress in masonry.

Table 2: The applied failure load value and the size of the places

Sample code	**13АЦ-0,1**	**13АЦ-0,14**	**13АЦ-0,24**
Dimensions of the sample h × b × l, mm	1050×250×1050	1050×250×1050	1050×250×1050
Load platform width l_{loc}, mm	100	150	250
Ultimate load F_u^{test}, kN	478	556	1000

Table 3: Outlines of samples

Sample code	Outline of sample
13АЦ-0,1	
13АЦ-0,14	
13АЦ-0,24	

The highest values of stresses σ_z have at the slightest load platform (l_{loc} = 100 mm) for the sample 13АЦ-0,1 equal to 19.46 MPa. The stresses have the smallest values for the sample 13АЦ-0,14 (l_{loc} = 150 mm) and are equal to 15.08 MPa.

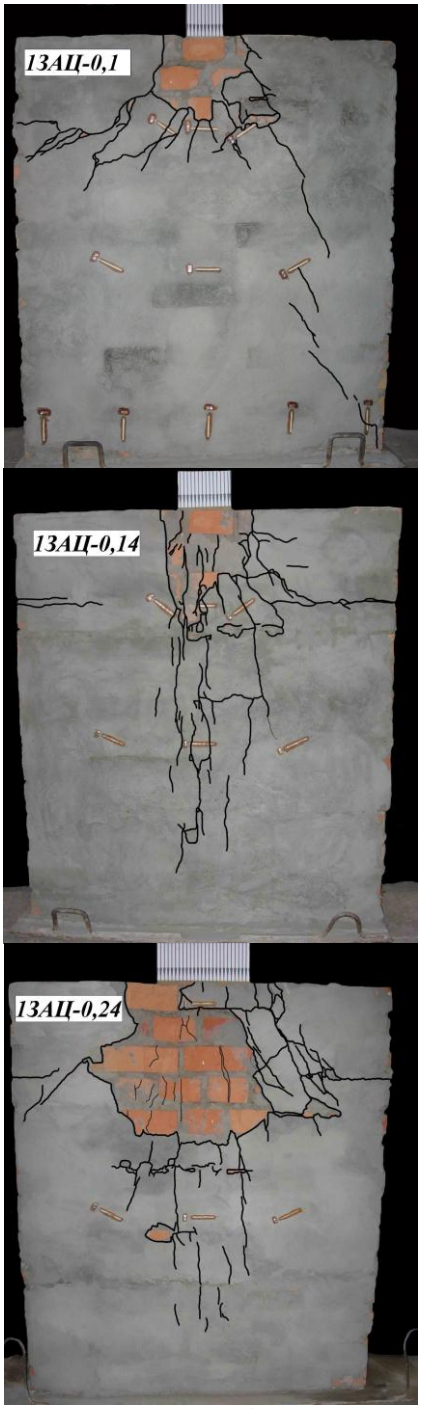


Fig. 3: Tested samples failure character

Normal stress σ_x toward the horizontal axis x of the specimen (along its long side) reaches the highest value in the sample 13АЦ-0,1 at l_{loc} = 100 mm and 18.52 MPa. The smallest of these stresses is in the sample 13АЦ-0,14 at l_{loc} = 150 mm and is equal to 13,96 MPa.

The tensile shear stress τ_{zx} in the *zx* plane is the largest for the sample 13АЦ-0,24 at l_{loc} = 250 mm and is equal to 5,03 MPa. The smallest of these stresses is in the sample 13АЦ-0,14 at l_{loc} = 150 mm and is equal to 4,43 MPa. The dispersion of these stresses is 11.9%.

The size of the stresses in the reinforcing bars has a slightly different character than the stresses on the masonry surface. Directly under local loading platform at the top mesh reinforcing bars tensile stress developes. As wider the loading platform, as longer is reinforcing bar working in the tension. They reach the maximum value in the sample 13АЦ-0,24. In these areas meshes width of the tensile stress increases, confirming theoretical spread angle under the load 45^0.

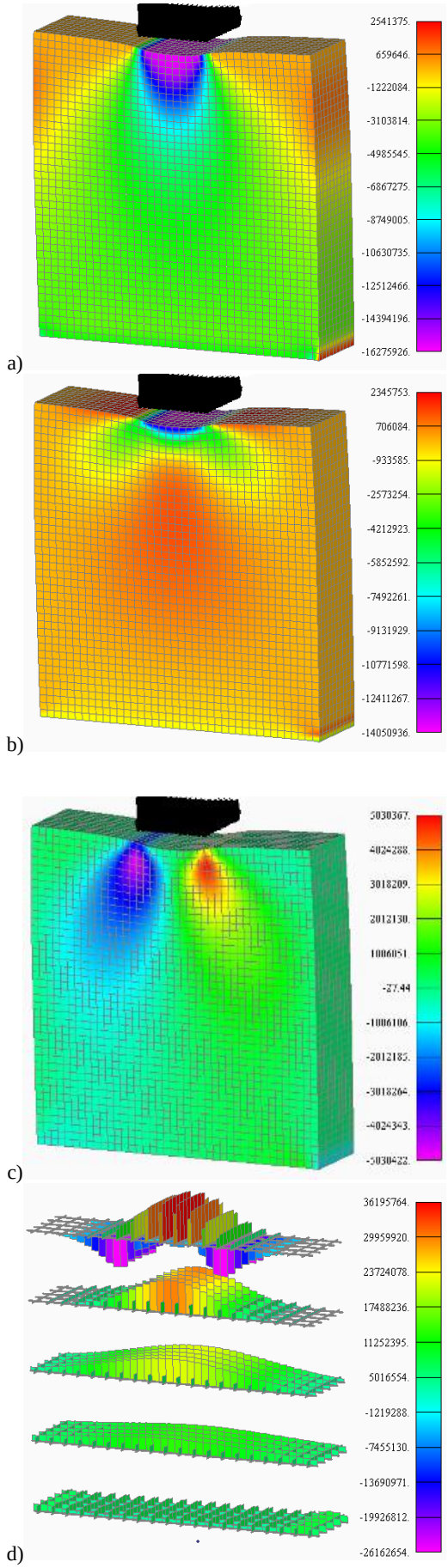


Fig. 4: Stress distribution (MPa) on the sample 13АЦ-0,24 surface: a) normal σ_z; b) normal σ_x; c) tangent τ_{zx} d) in the reinforcing meshes bars.

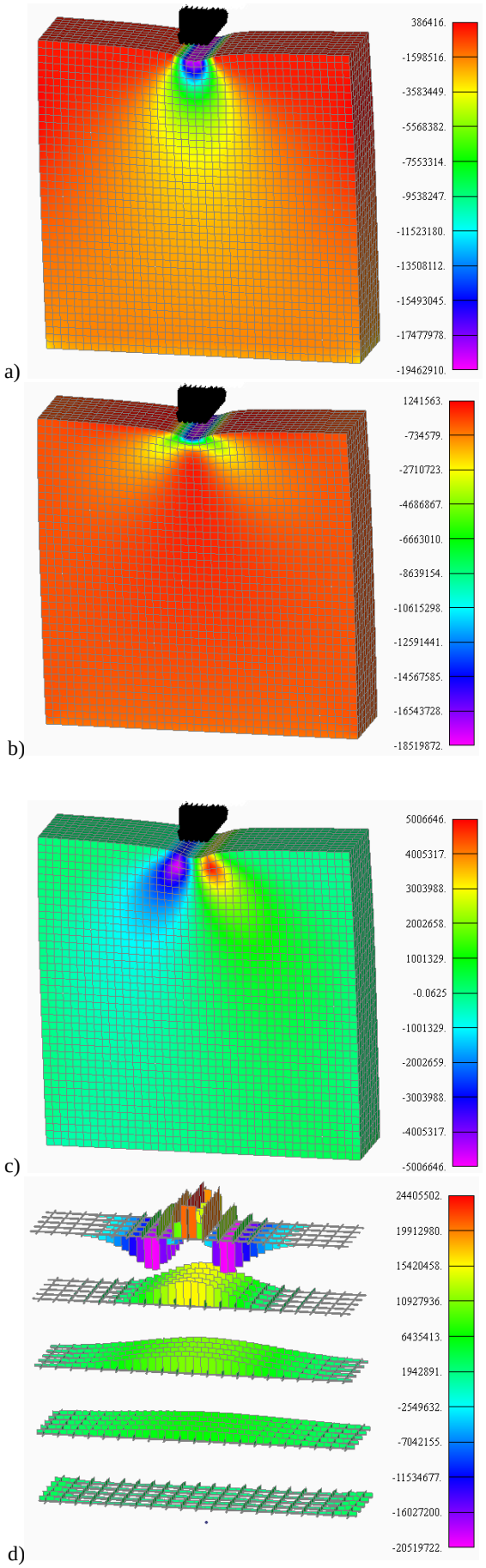


Fig. 5: Stress distribution (MPa) on the surface sample 13АЦ-0,1: a) normal σ_z; b) normal σ_x; c) tangent τ_{zx} d) in the reinforcing meshes bars.

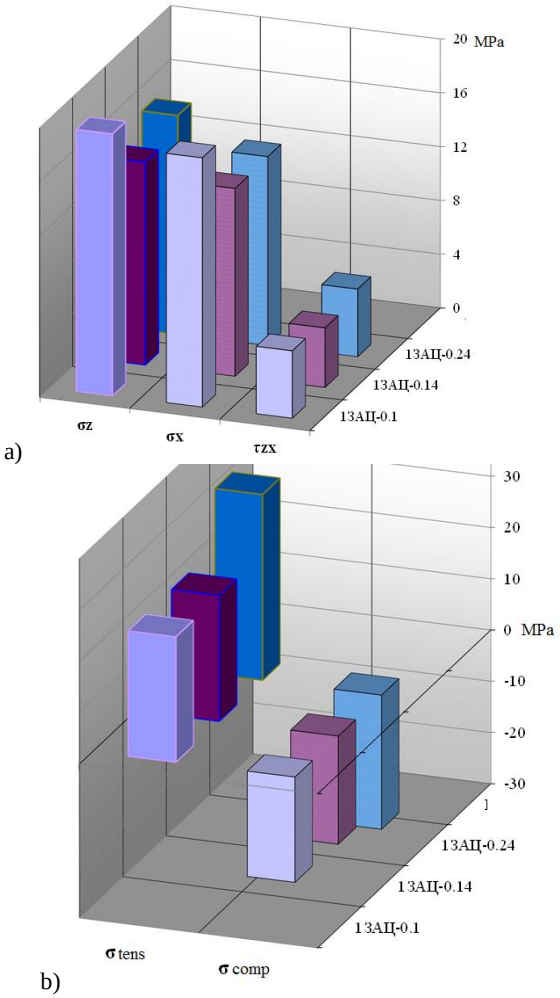


Fig. 6: Structure comparison histograms: a) on the surface of reinforced masonry samples; b) in reinforcing bars.

Near the tensile areas in the reinforcing bars of the upper meshes (outside the local load area), the concentric compression areas appear in the rods. The width of these areas is approximately equal to the stretching areas width. The maximum value of the compressive stresses in the bars also occurs in the sample 13АЦ-0,24.
In Table 4 we compare the experimental and numerically obtained values of the stresses σ_z normal toward the vertical axis z. In the last column, the percentages of these two values are calculated.

Table 4: Comparison of experimental and numerically obtained values of normal to vertical axis z load stresses σ_z.

№	Sample code	Dimensions of loading platform, mm	Ultimate load F_u^{test}, kN	The stresses on the masonry surface		
				σ_z^{test}, МПа	σ_z^{num}, МПа	$\Delta\sigma$, %
1	**13АЦ-0,1**	250×100	478	-19,12	-19,46	1,75
2	**13АЦ-0,14**	250×150	556	-14,83	-15,08	1,66
3	**13АЦ-0,24**	250×250	1000	-16,00	-16,28	1,72
					$\Delta\sigma$ =	1,71

3. Results of the Masonry Elements Stress-Strain State Modelling

A stress-strain state numerical investigation was performed on three models of clay masonry, the size and loading of which corresponded to experimentally tested ones. The samples are different in the width of the applied load and its value. Table 4 lists the values of the applied load and the size of the platforms to which this load was applied.

The deformations comparison in the reinforcing bars of the reinforcing masonry meshes received after the experimental tests (the indications on reinforcing bars) and the results of the numerical modelling was made. Below, in Figure 7, the comparison of the deformations for the upper and lower meshes only for the sample 13АЦ-0,14 is shown. The location of the indications on the reinforcing mesh is respectively shown on each graph.

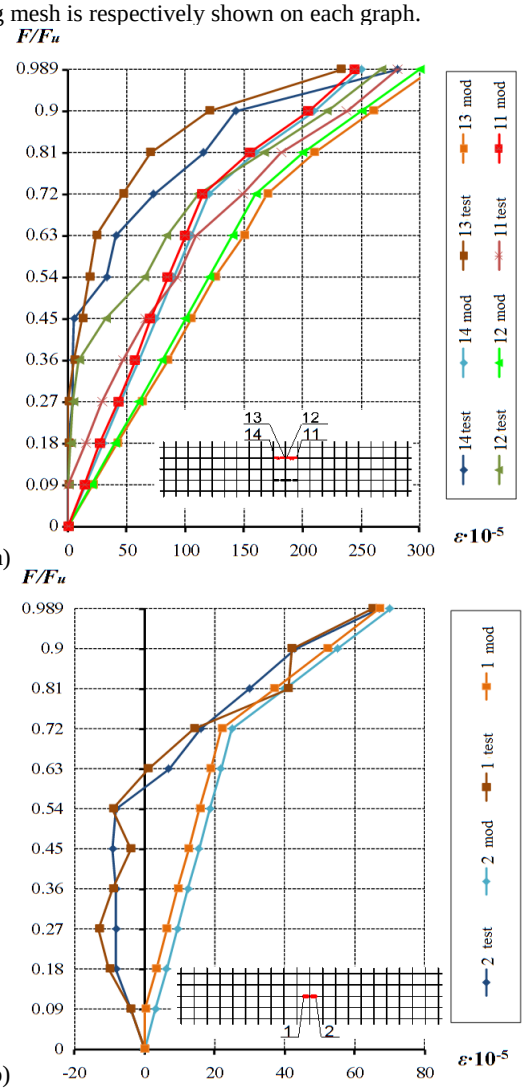


Fig. 7: Comparison of the «F/F_u–ε_s» relation for the sample 13АЦ-0,14 reinforcing meshes: a) upper; b) the lower one.

The diagrams (Figure 7) present a straight line dependence on the initial loading areas on graphs constructed on the basis of numerical modelling. This is due to the software system based in the Hooke's Law which is directly proportional to the "deformation-load". In general, the deformations obtained from the indicators during the experimental tests and the results of numerical modelling give a good convergence (the deviation is up to 24%).

4. Conclusion

Accepted models of building structures in the software complex are adequate and correspond to real constructions. Comparing the convergence of the results obtained from calculating models of various finite elements (tetrahedra and hexahedra) with different sizes, it is decided to divide the building constructions models of the correct geometric shape into hexaders with a side of 25 mm, which is approximately equal to 2.5% of the total height, or the studied model length. At such a finite-element grid, the values of normal stresses differed from the average value calculated on the basis of all calculations to 7.3%. The necessary resources of a personal computer to create and calculate such a model are suffi-

cient and suitable for studying the stress-strain state of simulated structures.

The modelling of the reinforced masonry elements stress-strain state allowed to identify places with maximum stresses and deformations. Priority attention during experimental investigation should be paid to them. The deformations obtained from the readings of the electric resonators during the experimental tests and according to the results of numerical modelling give a good convergence (the deviation is up to 24%).

References

[1] Zenkevich OS, Chang I. The method of finite elements in the theory of constructions and in the mechanics of continuous medium, 238 P. M.: Nedra (1974).

[2] Gasenko AV, Pigug OV, Magan IV: Modelling of the stress-strain state of the unassembled units of a monolithic reinforced concrete slab with steel-ton columns. SNAU Bulletin. Series: Construction, vol. 11 (14), pp. 53-60. Sumy (2010).

[3] Grinev VV. Analysis of strained-deformed state when compressing masonry from vibropressed concrete, cavernous stones using computer modelling. Zb sciences пр. "Resource-saving materials, constructions, buildings and structures", vol. 15, pp. 142-149. Rivne: NUVHtaP (2007).

[4] Musinova V, Ts. MSC / NASTRAN. User's Guide. - The MacNeal-Schwendler Corporation, 188 R. (1995).

[5] Dovzhenko OO, Pinchuk NM Strength of reinforced masonry under local loading, Technical sciences, from theory to practice, 2012. – Vol. 8, – P. 136-142.

[6] Hasenko AV, Yurko IA, Fenko OG., Yurko PA Causes of the eccentric compression reinforced concrete elements fixed joint stanchion and rafter gable frame of agricultural buildings // The International Scientific Periodical Journal "Modern Technology and Innovative Technologies". – Germany: Karlsruhe, 2017. – Issue №2, Vol.2. – pp. 126 – 129. – DOI: 10.21893/2567-5273.2017-02-02-033.

[7] Semko OV, Gasenko AV, Lazarev DM, Avramenko YuO Features of modelling of the stress-strain state of light steel thin-walled structures // Bulletin of DNUZT named after academician V. Lazaryan. - Dnipropetrovsk, 2011. - Vip. 39. - P. 191 - 194.

[8] Beicha D. Effective transverse elastic properties of unidirectional fiber reinforced composites [Text] / D. Beicha, T. Kanit, Y. Brunet, A. Imad, A. E. Moumen, Y. Khelfaoui // Mechanics of Materials. – 2016. – Vol. 102. – pp. 47-53. – DOI: 10.1016/j.mechmat.2016.08.010.

[9] Bishnu P. A new method of applying long-term multiaxial stresses in concrete specimens undergoing ASR, and their triaxial expansions [Text] / P. G. Bishnu, K. P. Daman // Materials and Structures. – 2016. – Vol. 49 (9). – pp. 3409-3508. – DOI: 10.1617/s11527-015-0734-z.

[10] Rychkov SP Modelling of Constructions in the Femap with NX Nastran. - M.: DMC Press, 2013. - 784 p.

[11] Dębski H, Koszałka G, Ferdynus M Application of fem in the analysis of the structure of a trailer supporting frame with variable operation parameters // Eksploatacja i Niezawodnosc – Maintenance and Reliability. 2012. – Vol. 14, № 2 – P. 107 – 114.

[12] Piskunov VG, Gorik A, Cherednikov VN Modeling of Transverse Shears of Piecewise Homogeneous Composite Bars Using an Iterative Process with Account of Tangential Loads. 2. Resolving Equations and Results Mechanics of Composite Materials November 2000, Vol. 36, Issue 6, pp 445–452 https://doi.org/10.1023/A:1006798314569